The Asymmetry of Chloride Transport at 38°C in Human Red Blood Cell Membranes

PHILIP A. KNAUF,* PEDER K. GASBJERG,‡ and JESPER BRAHM‡

From the *Department of Biophysics, University of Rochester Medical Center, Rochester, New York 14642; and ‡Department of Medical Physiology, The Panum Institute, University of Copenhagen, DK-2200 Copenhagen N, Denmark

ABSTRACT Band 3–mediated Cl^- exchange in human red blood cells and resealed ghosts was measured at 38°C by the continuous flow tube method. When external Cl^- concentration, $C^{(o)}$, is varied with constant internal Cl^- concentration, $C^{(i)}$, the flux fits a simple Michaelis-Menten saturation curve (MM fit), with $K_{1/2}^{o} = 3.8 \pm 0.4$ mM. When the Cl^- concentration is varied simultaneously at both sides of the membrane in resealed ghosts ($C^{(i)} = C^{(o)} = C^{(i=o)}$), the flux rises toward a flat maximum between 200 and 450 mM Cl^-, and then decreases at very high $C^{(i=o)}$. An MM fit to the data with $C^{(i=o)} < 500$ mM gives $K_{1/2}^{s}$ of 106 ± 13 mM; fits including modifier site inhibition (MS fit) give an over threefold higher $K_{1/2}^{s}$. Despite this uncertainty, the intrinsic asymmetry of unloaded transport sites, A (defined as $E^{(o)}/E^{(i)}$ with $C^{(i)} = C^{(o)}$, where $E^{(i)}$ is the fraction of unloaded inward-facing sites and $E^{(o)}$ is the fraction of unloaded outward-facing sites), calculated from $K_{1/2}^{s}$ and $K_{1/2}^{o}$, ranges only from 0.046 to 0.107. A new method, which uses the initial slope of a plot of Cl^- flux versus $C^{(i=o)}$, gives A values of 0.023 to 0.038. Flufenamic acid (FA) inhibits Cl^- exchange by binding to an external site different from the transport site. At 38°C, FA binds 24–36 times more tightly to $E^{(o)}$ than to $E^{(i)}$. Estimates of A from FA inhibitory potency range from 0.01 to 0.05. All methods, including bicarbonate data from the preceding paper, indicate that at 38°C, like 0°C, far more band 3 molecules are in the $E^{(i)}$ than in the $E^{(o)}$ form. The agreement of various methods supports the ping-pong model for anion exchange, and demonstrates that the intrinsic asymmetry is very slightly, if at all, affected by temperature.

KEY WORDS: band 3 • anion exchange • erythrocytes • flufenamic acid • ping-pong model

INTRODUCTION

As mentioned in the preceding paper (Gasbjerg et al., 1996), most data indicate that the one-for-one anion exchange (Brahm, 1977; Hunter, 1971; Hunter, 1977) mediated by the red blood cell protein known as band 3, capnophorin, or AE1 (Wieth and Bjerrum, 1983; Kopito, 1990; Cabantchik and Rothstein, 1974; Passow et al., 1974; Tanner et al., 1988; Lux et al., 1989) is accomplished by a ping-pong mechanism (Gunn and Fröhlich, 1979; Jennings, 1982; Knauf, 1989; Jennings, 1992*a*). In this model, capnophorin can exist in a form ($E^{(i)}$), in which the transport site faces the inside of the cell, or in a different form ($E^{(o)}$), in which the transport site faces the external medium. Transition from $E^{(o)}$ to $E^{(i)}$ or vice-versa only occurs when a transportable anion such as Cl^- is bound. Thus, anions are transported alternately in opposite directions, resulting in a one-for-one exchange process.

Capnophorin is structurally asymmetric, with different segments facing the inside or outside of the cell (Passow, 1986; Knauf, 1986; Jennings, 1992*b*). It is also functionally asymmetric. Gunn and Fröhlich (1979) showed that at 0°C, the asymmetry factor A, defined as $E^{(o)}/E^{(i)}$ for $C_{Cl}^{(i)} = C_{Cl}^{(o)}$,[1] is about 1/15. Thus, under conditions where $C_{Cl}^{(i)} = C_{Cl}^{(o)}$, about 15 times more unloaded transport sites are in the $E^{(i)}$ form than are in the $E^{(o)}$ form. The functional asymmetry of capnophorin has been determined at 0°C in several other studies for chloride (for a review, see Knauf and Brahm, 1989) and more recently also for bicarbonate (Gasbjerg and Brahm, 1991).

According to the ping-pong model, $A = kK_o/k'K_i$, where k and k' are the rate constants for the transition from inward-facing to outward-facing, or vice versa, and K_o and K_i are the true dissociation constants for substrate (e.g., Cl^-) binding at the outside and inside re-

Portions of this work have previously appeared in abstract form (Knauf, P.A., and J. Brahm. 1985. *Acta Physiol. Scand.* 124[Suppl. 542]:155; and Knauf, P.A., and J. Brahm. 1986. *Biophys. J.* 49:579*a*).

Address correspondence to Philip A. Knauf, Ph.D., Department of Biophysics, University of Rochester Medical Center, Rochester, NY 14642. Fax: 716-275-6007; E-mail:knau@db1.cc.rochester.edu

[1]*Abbreviations used in this paper:* $C^{(i)}$ or $C_{Cl}^{(i)}$, intracellular chloride concentration; $C^{(o)}$ or $C_{Cl}^{(o)}$, extracellular chloride concentration; $C^{(i=o)}$ or $C_{Cl}^{(i=o)}$, chloride concentration when internal bichloride equals external bichloride; FA, flufenamic acid; $J^{fl,o}$, actual unidirectional efflux (asymmetric conditions where $C^{(o)}$ varies); $J_{max}^{eff,o}$, maximum unidirectional efflux (asymmetric conditions where $C^{(o)}$ varies); $J_{max}^{eff,s}$, maximum unidirectional efflux (symmetric conditions); $J^{eff,s}$, actual unidirectional efflux (symmetric conditions); K_i, self-inhibition dissociation constant (symmetric conditions); $K_{1/2}^{i}$, inside half-saturation constant (asymmetric conditions where $C^{(i)}$ varies); $K_{1/2}^{o}$, outside half-saturation constant (asymmetric conditions where $C^{(o)}$ varies); $K_{1/2}^{s}$, overall half-saturation constant (symmetric conditions); NMR, nuclear magnetic resonance.

 J. GEN. PHYSIOL. © The Rockefeller University Press • 0022-1295/96/12/577/13 $2.00
Volume 108 December 1996 577–589

spectively. The asymmetry can be due either to differences between k and k', or between K_o and K_i, or both.

Regardless of which is the case, the ping-pong model predicts that the value of A should be independent of the transported substrate. Gasbjerg and Brahm (1991) found that the values of A calculated from chloride or bicarbonate data at 0°C were very similar (0.05–0.12), as predicted by the ping-pong model.

In the present study, to see whether or not the asymmetry observed at 0°C persists under more physiological conditions, we have determined A from measurements of chloride transport at 38°C, performed with the continuous flow tube technique, which is well-suited to measure rapid transport processes (Brahm, 1977; 1989). Together with the results of the preceding paper (Gasbjerg et al., 1996), these data allow us to test the prediction of the ping-pong model that A should be the same for Cl^- as for HCO_3^-. To further examine the model's predictions, we have used the noncompetitive inhibitor, flufenamic acid (FA), to test the values of A obtained by flux measurements.

Theory

For a simple ping-pong model, the saturation of the transport system with external Cl^- fits a Michaelis-Menten equation as follows:

$$J^{eff,o} = J^{eff,o}_{max} \cdot C^{(o)}_{Cl} / (K^{o}_{1/2} + C^{(o)}_{Cl}). \quad (1)$$

An analogous equation is obtained for saturation with internal Cl^-.

When $C^{(o)}_{Cl}$ and $C^{(i)}_{Cl}$ are both varied in parallel, a similar Michaelis-Menten saturation equation is obtained:

$$J^{eff,s} = J^{eff,s}_{max} \cdot C^{(i=o)}_{Cl} / (K^{s}_{1/2} + C^{(i=o)}_{Cl}). \quad (2)$$

If internal Cl^- inhibits transport by binding to a second "modifier" site (Dalmark, 1976; Knauf and Mann, 1986), the flux equation for a symmetrical variation of chloride concentrations becomes (Gasbjerg and Brahm, 1991):

$$J^{eff,s} = J^{eff,s}_{max} \cdot C^{(i=o)}_{Cl} / [(K^{s}_{1/2} + C^{(i=o)}_{Cl}) \cdot (1 + C^{(i=o)}_{Cl}/K_I)], \quad (3)$$

where K_I is the concentration of internal Cl^- required to half-saturate the modifier site.

The asymmetry factor, A, is given by:

$$A = K^{o}_{1/2} \cdot (1 + K^{s}_{1/2}/C^{(i)}_{Cl}) / (K^{s}_{1/2} - K^{o}_{1/2}), \quad (4)$$

where $C^{(i)}_{Cl}$ is the (constant) internal Cl^- concentration at which $K^{o}_{1/2}$ is measured (Knauf and Brahm, 1989).

In the case where $K^{s}_{1/2}$ is difficult to determine, for example, because of modifier site inhibition, an alternate approach can be used to obtain A as follows: From Eqs. A6a and A6b of Gasbjerg and Brahm (1991):

$$K^{o}_{1/2} / J^{eff,o}_{max} = A / (E_t \cdot D), \quad (5)$$

where E_t is the total amount of band 3 present, and D is a combination of constants as defined in Gasbjerg and Brahm (1991).

Similarly, under symmetric conditions ($C^{(i)}_{Cl} = C^{(o)}_{Cl} = C^{(i=o)}_{Cl}$), from Eq. A8a and A8b of Gasbjerg and Brahm (1991):

$$K^{s}_{1/2} / J^{eff,s}_{max} = (A + 1) / (E_t \cdot D). \quad (6)$$

Combining Eq. 5 and 6, we can define R as:

$$R = (K^{o}_{1/2} / J^{eff,o}_{max}) / (K^{s}_{1/2} / J^{eff,s}_{max}) = A / (A + 1). \quad (7)$$

Thus, we can solve for A in terms of R:

$$A = R / (1 - R) \quad (8)$$

$K^{s}_{1/2} / J^{eff,s}_{max}$ can be determined as follows: If there is inhibition by Cl^- at an internal modifier site, Eq. 3 gives $J^{eff,s}$ as a function of $C^{(i=o)}_{Cl}$. As $C^{(i=o)}_{Cl}$ approaches zero, or more properly as long as $C^{(i=o)}_{Cl} \ll K^{s}_{1/2}$ and $C^{(i=o)}_{Cl} \ll K_I$, Eq. (3) becomes:

$$J^{eff,s} = J^{eff,s}_{max} \cdot C^{(i=o)}_{Cl} / K^{s}_{1/2}. \quad (9)$$

Thus, $K^{s}_{1/2} / J^{eff,s}_{max}$ can be determined from the reciprocal of the slope of a plot of $J^{eff,s}$ as a function of $C^{(i=o)}_{Cl}$. The criterion for applicability of Eq. (9) is that $C^{(i=o)}_{Cl}$ is low enough so that $J^{eff,s}$ is linearly dependent on $C^{(i=o)}_{Cl}$.

The values of $K^{o}_{1/2}$ and $J^{eff,o}_{max}$ can be obtained from saturation curves at any fixed value of $C^{(i)}_{Cl}$. A problem arises, however, if high values of $C^{(i)}_{Cl}$ are used, because self-inhibition by internal Cl^- reduces the observed $J^{eff,o}_{max}$, $J^{eff,o}_{max}(meas)$, but does not affect the observed $K^{o}_{1/2}$ (based on the assumption that binding of internal Cl^- to the modifier site is not affected by the orientation of the transport site). Thus,

$$1/J^{eff,o}_{max}(true) = (1/J^{eff,o}_{max}(meas)) / (1 + C^{(i)}_{Cl}/K_I), \quad (10)$$

so R in Eq. 8 should be divided by $(1 + C^{(i)}_{Cl}/K_I)$ in order to obtain the true value of A (Gasbjerg and Brahm, 1991). In practice, this correction is somewhat difficult to apply, because of the uncertainty in the value of K_I.

MATERIALS AND METHODS

Media

The following media (mM) were prepared from reagent grade chemicals: A. 150 KCl, 0.5 KH_2PO_4; B. 165 KCl, 2 KH_2PO_4; C. 2–600 KCl, 0.5–2 KH_2PO_4 with either sucrose, citrate-sucrose (Gunn and Fröhlich, 1979), or gluconate to replace KCl below 150 mM.

Preparation of Red Blood Cells and Ghosts

Human red cells, which were drawn into heparin, were washed once in Medium A or B.

Red blood cells. Red blood cells were titrated to pH 7.2 at 38°C with either CO_2 or 0.1 M KOH. The cells were subsequently washed three additional times in the titrated stock solution, and

resuspended to a hematocrit of ≈50% for incubation with isotope (see below).

Red cell ghosts. Red cell ghosts with various $C_{Cl}^{(i)}$ were prepared as described previously (Gasbjerg and Brahm, 1991; Knauf and Brahm, 1989).

Inhibition

Flufenamic acid (FA; Aldrich Chemical Co., Milwaukee, WI), dissolved in ethanol, was added to the efflux medium at the desired concentration. When FA was used in an experiment, all flux solutions contained a total of 1% ethanol. FA was kept in the dark and the experiments were performed in dim light.

Incubation with Isotope, and Determinations of Radioactivity and Cell Water Content

The red cells or ghosts were incubated in medium C at the desired $C_{Cl}^{(o)}$ with $^{36}Cl^-$ (AEK, Risø, Denmark), ≈18 kBq (0.5 μCi) per ml cell suspension at a cytocrit of ≈50%. For FA fluxes, cells were incubated with 0.3 μCi/ml carboxyl-^{14}C-FA (Research Products International, Mount Prospect, IL) in 150 mM Cl^- medium with 10 μM FA and 1% ethanol. The cells or ghosts were isolated by centrifugation at 20,000 rpm (Sorvall RC-5 centrifuge; DuPont Instruments-Sorvall Biomedical Div., Newtown, CT) in nylon tubes for determination of tracer distribution and cell water content, and in 6-ml tubes for efflux experiments with the continuous flow tube method.

The radioactivity of the cells and the supernatant was determined by liquid β-scintillation spectrometry after precipitation with 7% (vol/vol) perchloric acid. The radioactivity of cell-free filtrates and centrifuged "infinity" samples from the efflux experiments (see *Determination of the Efflux Rate* section) was measured without a preceding precipitation.

Determination of water content was carried out in red cells by drying a cell sample to constant weight (Dalmark and Wieth, 1972), and in ghosts by Coulter counting (Coulter Counter model DN; Coulter Electronics, Inc., Hialeah, FL), correcting for trapped extracellular volume (2% in red blood cell samples and 8% in red cell ghost samples).

Determination of the Efflux Rate

All experiments were carried out by means of the continuous flow tube method (Brahm, 1977; 1989) by measuring the rate of the unidirectional efflux of $^{36}Cl^-$ from preloaded cells into isotope-free medium C at a hematocrit of ≤0.5%. Rate constants for exchange were calculated from a two compartment model, as previously described (Brahm, 1977; Gasbjerg and Brahm, 1991; Knauf and Brahm, 1989). In experiments with high internal and very low external chloride concentrations ($C_{Cl}^{(o)} < 5$ mM), the measured exchange rate constant was adjusted according to the amount of Cl^- in the internal and external compartments as previously described (Knauf et al., 1989).

The unidirectional efflux of radioactively labeled chloride, J_{Cl}^* (mol cm^{-2} s^{-1}), is defined by:

$$J_{Cl}^* = k_{Cl}^* \cdot V_c/A_c \cdot C_{Cl}^{(i)*} = P_{Cl}^* \cdot C_{Cl}^{(i)*}, \qquad (11)$$

where k_{Cl}^* (s^{-1}) is the rate coefficient for tracer efflux, V_c (cm^3) is the cell water volume, A_c is the cell membrane area ($1.42 \cdot 10^{-6}$ cm^2 per cell, see Brahm (1982)), $C_{Cl}^{(i)*}$ is the cell tracer concentration (mol cm^{-3}), and P_{Cl}^* is the tracer permeability (cm s^{-1}). Under the assumption that the anion transporter does not distinguish between $^{36}Cl^-$ and Cl^- under a given set of conditions, we used P_{Cl}^* to calculate the unidirectional efflux of non-radioactive chloride, J^{eff}.

Curve Fitting

The fitting of mathematical functions describing simple Michaelis-Menten kinetics (MM, Eqs. 1 and 2) or with inclusion of a modifier site (MS, Eq. 3) to the experimental data was performed using nonlinear least-squares regression analysis with Sigmaplot (Jandel Scientific, Corte Madesa, CA). IC_{50} values were determined from a nonlinear fit of the equation for hyperbolic (single site) inhibition to the flux versus inhibitor concentration data, using either Enzfitter (Elsevier Biosoft) or Sigmaplot. Lines on reciprocal plots were drawn using the parameters from these nonlinear fits. Error values are SEM.

RESULTS

Strategy for Determination of the Asymmetry Factor, A

An experimentally straightforward way (*Theory*, Eq. 4) to measure A is to keep $C_{Cl}^{(i)}$ constant and vary $C_{Cl}^{(o)}$ to determine $K_{1/2}^o$, and then to vary $C_{Cl}^{(i)}$ and $C_{Cl}^{(o)}$ ($C_{Cl}^{(i=o)}$) simultaneously to obtain the symmetric half-saturation constant $K_{1/2}^s$. As $C_{Cl}^{(o)}$ is varied, a proper substituent must be used in order to maintain constant osmolality and cell volume. When $C_{Cl}^{(i=o)}$ varies, ionic strength also varies. Both factors should be considered as potential sources of error in determining A.

Internal Chloride Is Constant, External Chloride Varies

Fig. 1 shows the Cl^- exchange fluxes calculated from continuous flow tube measurements of Cl^- exchange rate constants in intact red cells with an average $C_{Cl}^{(i)}$ ($\langle C_{Cl}^{(i)} \rangle$) of 105.4 mM suspended in media with different $C_{Cl}^{(o)}$ at pH 7.2, with sucrose replacing Cl^-. The Cl^- flux saturates at relatively low $C_{Cl}^{(o)}$, and there is no indication of a decrease in flux at very high $C_{Cl}^{(o)}$, as at 0°C

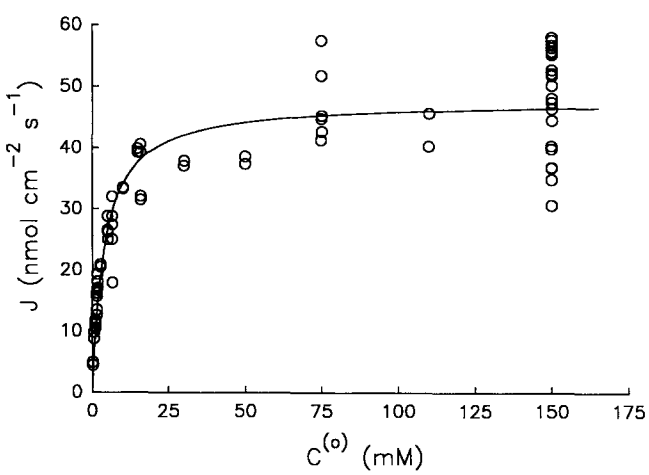

FIGURE 1. Unidirectional chloride efflux from intact red cells at 38°C as a function of external Cl^-. Flux was determined as described in MATERIALS and METHODS. The pH was 7.2, and sucrose was used to replace Cl^-. The average $C_{Cl}^{(i)}$ was 105.4 ± 6.3 mM (n = 22). The solid line represents a Michaelis-Menten (MM) fit (Eq. 1) to the data, with $J_{max}^{eff,o}$ = 47.7 nmol cm^{-2} s^{-1} and $K_{1/2}^o$ = 4.04 mM.

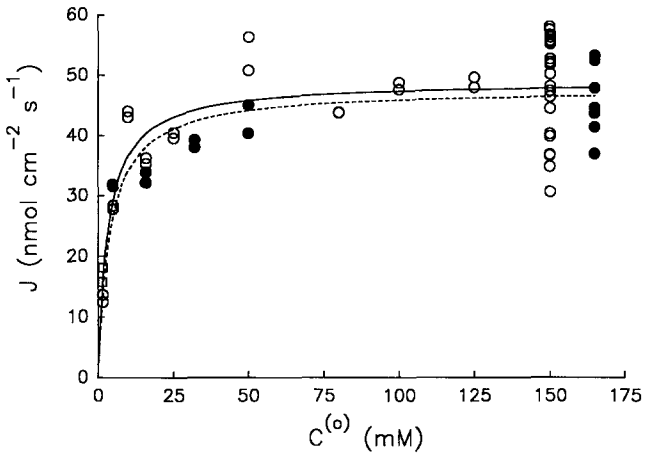

FIGURE 2. Dependence of unidirectional Cl^- efflux on external Cl^- concentration in cells with constant external ionic strength or in ghosts. Conditions as in Fig. 1. Open circles represent data for intact cells ($C_{Cl}^{(i)}$ = 104.6 ± 6.5 mM, n = 13) with gluconate substituted for external Cl^-; open squares are with citrate-sucrose replacing Cl^-, and solid circles are for ghosts ($C_{Cl}^{(i)}$ = 174.7 ± 4.5 mM) with sucrose replacing external Cl^-. The solid line represents the MM best fit to the intact cell data with gluconate replacing external Cl^-, with $J_{max}^{eff,o}$ = 49.0 nmol cm^{-2} s^{-1} and $K_{1/2}^{o}$ = 3.42 mM. The dashed line shows the best fit to the intact cell data with sucrose replacing external Cl^-, from Fig. 1.

(Gasbjerg and Brahm, 1991). A nonlinear least squares fit to the Michaelis-Menten (MM) equation (*solid line*) gives $J_{max}^{eff,o}$ of 47.7 ± 1.2 nmol cm^{-2} s^{-1} and $K_{1/2}^{o}$ of 4.04 ± 0.55 mM.

In Fig. 1, there is a considerable decrease in ionic strength at the lowest values of $C_{Cl}^{(o)}$, which might alter $K_{1/2}^{o}$. To avoid this, in Fig. 2 gluconate was used to maintain constant ionic strength when $C_{Cl}^{(o)}$ was varied. The MM fit in this case (*solid line*) gives $J_{max}^{eff,o}$ of 49.0 (±1.5) nmol cm^{-2} s^{-1} and $K_{1/2}^{o}$ of 3.42 (±0.95) mM, very similar to the values obtained with sucrose replacing Cl^- (*dashed line*, showing best fit from Fig. 1).

At 0°C gluconate inhibits Cl^- exchange, probably by a competitive mechanism, with a dissociation constant for binding to the external-facing transport site of about 50 mM (Knauf and Mann, 1986). To see whether or not gluconate significantly inhibits Cl^- exchange at 38°C, Cl^- efflux was measured at 1.5, 5, or 70 mM $C_{Cl}^{(o)}$, with sucrose or gluconate replacing Cl^-. At 5 and 70 mM $C_{Cl}^{(o)}$, no significant inhibition was seen with gluconate ≥100 mM; for 1.5 mM $C_{Cl}^{(o)}$, the apparent IC_{50} (concentration which gives half-inhibition) was 450 (±140) mM. As the concentration of gluconate in the medium never exceeded 149 mM, inhibition by gluconate should not significantly affect the fluxes at $C_{Cl}^{(o)} \geq 5$ mM.

The open squares show results in which 25 mM citrate, together with sucrose, was used to maintain ionic strength (Gunn and Fröhlich, 1979). Again, the fluxes are very similar to those with sucrose or gluconate. Thus, changes in external ionic strength seem to have no substantial effect on Cl^- exchange or on $K_{1/2}^{o}$. Because there were no apparent differences between the data with gluconate or citrate substitution and those with sucrose, the data sets can be combined. The MM fit to all of the cell data, with $\langle C_{Cl}^{(i)} \rangle$ of 105.9 ± 7.1 mM (n = 24), gives $J_{max}^{eff,o}$ of 48.2 ± 1.0 nmol cm^{-2} s^{-1} and $K_{1/2}^{o}$ of 3.83 ± 0.44 mM.

To ensure that the external Cl^- saturation data for intact cells can be compared with the data for $C_{Cl}^{(i)} = C_{Cl}^{(o)} = C_{Cl}^{(i=o)}$, which were obtained with resealed red cell ghosts, in Fig. 2 we compared the $C_{Cl}^{(o)}$ saturation in ghosts (with $C_{Cl}^{(i)}$ = 174.7 ± 4.5 mM, *solid circles*) with the data for cells (*open circles* and *best-fit lines*). Although there are fewer data points for ghosts, a MM fit gives $J_{max}^{eff,o}$ of 45.3 (±1.8) nmol cm^{-2} s^{-1} and $K_{1/2}^{o}$ of 3.01 (±1.03) mM, very similar to the parameters obtained with intact cells. Thus, at 38°C, as at 0°C (Funder and Wieth, 1976), the absence of intracellular constituents such as ATP from resealed ghosts seems to have no significant effect on anion exchange.

To be sure that valid comparisons could be made with the bicarbonate data from the preceding paper (Gasbjerg et al., 1996), which were obtained at the slightly higher pH of 7.8, we also measured the dependence of Cl^- exchange on external Cl^- in resealed ghosts at this pH (Fig. 3). The best fit to the MM equation (*solid line*) gives $J_{max}^{eff,o}$ of 54.0 (±1.5) nmol cm^{-2} s^{-1} and $K_{1/2}^{o}$ of 4.10 (±0.55) mM. The similarity of these values to those at pH 7.2 indicates that the transport system is homogeneous with respect to titration state within this pH range at 38°C.

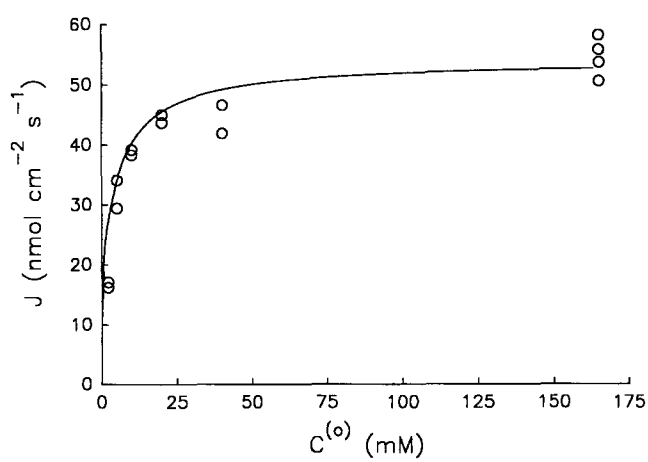

FIGURE 3. Effect of external Cl^- concentration on unidirectional Cl^- efflux from resealed ghosts at pH 7.8. Conditions are similar to those for ghosts in Fig. 2, except that the pH was 7.8. The solid line represents the best fit of the MM equation (Eq. 1) to the data. Parameters for the fit are given in the text.

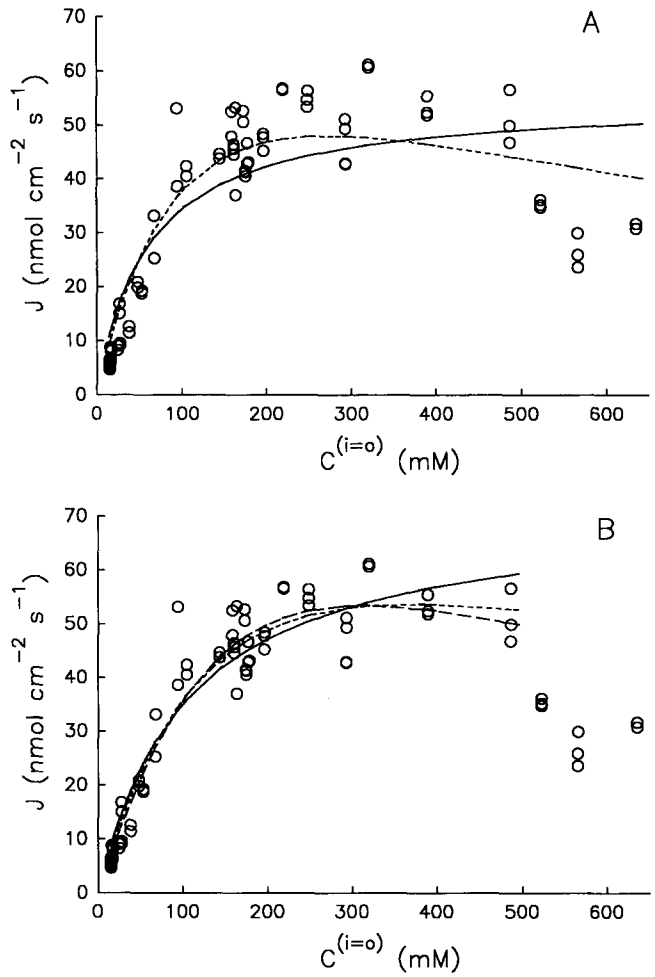

FIGURE 4. Dependence of Cl^- exchange flux on Cl^- concentration under symmetric conditions ($C^{(i)} = C^{(o)} = C^{(i=o)}$). Fluxes were measured at 38°C and pH 7.2 in resealed ghosts as described in MATERIALS AND METHODS. (*A*) The solid line represents a least squares best fit to all of the data with the MM equation (Eq. 2), with $K_{1/2}^s = 60 \pm 12$ mM and $J_{max}^{eff,s} = 55.1 \pm 2.9$ nmol cm^{-2} s^{-1}, while the dashed line shows the best fit to the MS equation (Eq. 3), with $K_{1/2}^s = 272$ mM, $K_I = 273$ mM, and $J_{max}^{eff,s} = 192$ nmol cm^{-2} s^{-1}. (*B*) Best fit lines are shown for the data with $C^{(i=o)} < 500$ mM for the MM model (*solid line*: $K_{1/2}^s = 106 \pm 13$ mM and $J_{max}^{eff,s} = 72.0 \pm 3.3$ nmol cm^{-2} s^{-1}), for the MS model (*short dashed line*: $K_{1/2}^s = 375$ mM, $K_I = 370$ mM and $J_{max}^{eff,s} = 216$ nmol cm^{-2} s^{-1}, all with SEM > the parameter values), and for a model (CMS) in which Cl^- binds to the modifier site only when Cl^- is bound to the transport site (*long dashed line*: $K_{1/2}^s = 334 \pm 136$ mM, $K_I = 297 \pm 158$ mM, and $J_{max}^{eff,s} = 167 \pm 53$ nmol cm^{-2} s^{-1}).

Symmetric Variation of Internal and External Chloride

The other piece of information needed to calculate the asymmetry factor, A (see Eq. 4) is $K_{1/2}^s$, the concentration of Cl^- which half-saturates the transport system when $C_{Cl}^{(i)} = C_{Cl}^{(o)} = C_{Cl}^{(i=o)}$. This was determined by preparing resealed red cell ghosts with different $C_{Cl}^{(i)}$, and then measuring Cl^- exchange in media with the same chloride concentration. From the results in Fig. 4 *A* it is apparent that the concentration of Cl^- required to saturate the transport system is much larger under these conditions than when $C_{Cl}^{(o)}$ alone is varied. Also, particularly at $C_{Cl}^{(i=o)} > 500$ mM, the flux decreases with increasing Cl^- concentration.

If we attempt to fit a simple MM equation to the data in Fig. 4 *A* (*solid line*), the fit is not very good and a value of 60 ± 12 mM is obtained for $K_{1/2}^s$, with $J_{max}^{eff,s}$ of 55 ± 3 nmol · cm^{-2} · s^{-1}. Use of the modifier site (MS) equation gives a slightly better fit (*dashed line*), with $K_{1/2}^s$ of 272 mM, K_I (for binding to the modifier site) of 273 mM, and $J_{max}^{eff,s}$ of 192 nmol · cm^{-2} · s^{-1}, but the line fits poorly to the points >500 mM and the standard errors for the parameters are enormous. A model in which Cl^- binds to the modifier site only when Cl^- is bound to the transport site (CMS) also gives a poor fit, with very large parameter errors. A number of other models, that included partial inhibition or monomer-monomer interactions, also failed to fit the high Cl^- data. It seems that the sharp drop in flux at $C_{Cl}^{(i=o)} > 500$ mM (which is statistically significant, $P < 0.01$ compared to the data from 200 to 500 mM) can only be explained by a model in which small changes in $C_{Cl}^{(i=o)}$ in the region >500 mM have a very large effect on

TABLE I

Determination of Asymmetry from $K_{1/2}^o$ and $K_{1/2}^s$

Data	$K_{1/2}^s$ (mM)*	$J_{max}^{eff,s}/K_{1/2}^s$	A‡	$1/A$	NSSR‖
MM fits:					
All	60 ± 12	0.915	0.107	9.4	83.5
<500	106 ± 13	0.678	0.075	13.3	46.6
<300	128 ± 20	0.618	0.068	14.7	46.4
<200	165 ± 32	0.555	0.061	16.4	37.4
<150	395 ± 173	0.473	0.046	21.6	23.9
MS Fits:					
All	271§	0.706	0.051	19.6	60.4
K_I =	273§				
<500	375§	0.576	0.047	21.3	40.7
K_I =	370§				
CMS Fits:					
All	1,913§	0.449	0.038	26.1	50.3
K_I =	31§				
<500	334 ± 136	0.500	0.048	20.8	39.6
K_I =	297 ± 158				

*Determined from the data ranges (in mM Cl^-) using Eq. 2 for MM fit and Eq. 3 for MS fit. For the CMS fit, assuming that Cl^- binds to the modifier site only when Cl^- is bound to the transport site, the following equation was used to fit the data:

$$J_{max}^{eff,s} = J^{eff,s}/(1 + K_{1/2}^s/C^{(i=o)} + C^{(i=o)}/K_I).$$

‡Determined from Eq. 4 in *Theory*, using $K_{1/2}^o = 3.83$ mM for $C_{Cl}^{(i)} = 105.9$ mM, obtained by fitting all of the intact cell data to the MM equation (Eq. 1). §Standard errors determined with Sigmaplot were larger than the parameter values. ‖Normalized sum of squares of residuals, obtained by taking the square root of the sum of the squares of the differences between the experimental and calculated values for each point; minimum value indicates best fit.

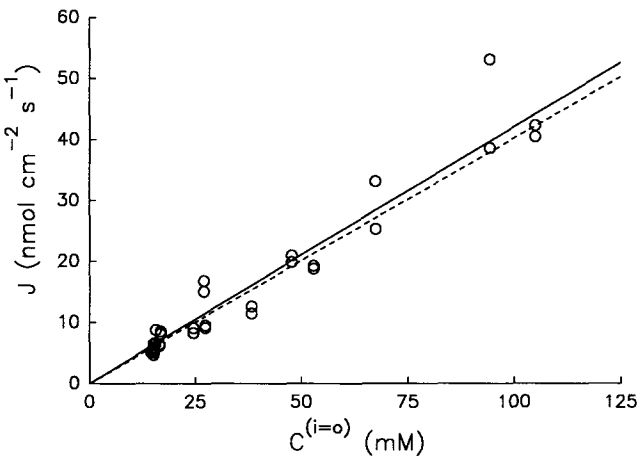

FIGURE 5. Effect of symmetric variation of Cl^- concentration on Cl^- exchange flux at low Cl^- concentrations. The same data for red cell ghosts shown in Fig. 4 are fitted to straight lines with a zero intercept in the range of low Cl^- concentrations. For the data with $C^{(o)} \leq 105$ mM, the best fit is shown by the solid line, whose slope is 0.421 ± 0.012 nmol cm^{-2} s^{-1} mM^{-1}; for $C^{(o)} \leq 70$ mM, the best fit is shown by the dashed line, with slope of 0.402 ± 0.013 nmol cm^{-2} s^{-1} mM^{-1}. Fits without assuming a zero y-intercept gave similar slopes, 0.436 ± 0.020 and 0.409 ± 0.025 nmol cm^{-2} s^{-1} mM^{-1}, respectively, with y-intercepts of -0.82 ± 0.87 and -0.25 ± 0.78 nmol cm^{-2} s^{-1}, neither of which was significantly different from zero.

transport. As such effects are difficult to model and have little relevance to the behavior of the system in the range of lower Cl^- concentrations, we chose to fit the model to the data in the range from 0 to 500 mM, excluding the points at very high Cl^-.

If we limit the data to $C_{Cl}^{(i=o)} < 500$ mM (Fig. 4 *B*), a MM fit gives $J_{max}^{eff,s}$ of 72 ± 3 nmol · cm^{-2} · s^{-1}, $K_{1/2}^s$ of 106 ± 13 mM (*solid line*), with a normalized sum of squares of residuals (NSSR) of 46.6. Either the MS (*short dashes*) or the CMS (*long dashes*) models give slightly lower NSSR (40.7 or 39.6, respectively), but the lines are almost indistinguishable from the MM fit throughout most of the data range (Fig. 4 *B*) and the parameter value errors are >30% of the values (Table I). Thus, the evidence that significant modifier site inhibition exists at $C_{Cl}^{(i=o)} < 500$ mM is weak. Gasbjerg and Brahm (1991) avoided the problem of high $C_{Cl}^{(i=o)}$ inhibition by fitting the simple MM equation to a more restricted data range, where modifier site effects are less apparent. Table I and Figs. 4 *A* and 5, however, show that as the range of $C_{Cl}^{(i=o)}$ decreases, there is little curvature in the plot of flux versus $C_{Cl}^{(i=o)}$ so increasingly large $K_{1/2}^s$ values are obtained, soaring to absurdly high (>1 M) levels when $C_{Cl}^{(i=o)}$ is restricted to 0–110 mM. For this data set, it seems impossible to specify a data range for which a "true" value of $K_{1/2}^s$ is obtained. Perhaps the only safe thing that can be said is that $K_{1/2}^s$ must be at least as large as the lowest value in Table I.

Determination of Asymmetry Factor, A

It might be thought that the difficulties in measuring $K_{1/2}^s$ precisely would preclude the possibility of determining *A*, since *A* depends on $K_{1/2}^s$ (see *Theory* section). However, when $K_{1/2}^s \gg K_{1/2}^o$, the dependence of *A* on $K_{1/2}^s$ is weak. As shown in Table I, despite the large variations in $K_{1/2}^s$, the calculated values of *A* range only from 0.046 to 0.107. Thus, at body temperature the asymmetry in unloaded site distribution seems to be similar to that at 0°C, with at least 10 times as many sites facing inward as facing outward (Knauf and Brahm, 1989; Gasbjerg and Brahm, 1991).

As described in the *Theory* section, a different approach can be used to determine *A*, without requiring a precise value of $K_{1/2}^s$. If $C_{Cl}^{(i=o)} \ll K_{1/2}^s$ and K_I, the plot of $J^{eff,s}$ versus $C_{Cl}^{(i=o)}$ is nearly linear with a slope equal to $J_{max}^{eff,s} / K_{1/2}^s$. Fig, 5 shows linear fits to the data for ghosts with symmetrical Cl^- concentrations for $C_{Cl}^{(i=o)} \leq 70$ mM or ≤ 105 mM. In both cases, linear fits with a zero y-intercept are very good (*dashed* or *solid lines*, respectively), with slopes of 0.402 or 0.421 nmol · cm^{-2} · s^{-1} · mM^{-1}. If the y-intercept is not constrained to be zero, similar fits are obtained with y-intercept values which are negative, but not significantly different from zero.

The reciprocal of the slope, combined with the values of $K_{1/2}^o$ and $J_{max}^{eff,s}$ obtained from the experiments in which $C_{Cl}^{(o)}$ was varied, was used to calculate the *A* values shown in Table II (see *Theory*). The *A* values for all combinations of the measured parameters fall in a very narrow range, from 0.029 to 0.038, indicating that there are 26 to 35 times as many inward-facing as outward-facing empty transport sites. If the effects on $J_{max}^{eff,o}$ of self-

TABLE II

Determination of Asymmetry from $K_{1/2}^o / J_{max}^{eff,o}$ and $K_{1/2}^s / J_{max}^{eff,s}$

$K_{1/2}^o / J_{max}^{eff,o}$	Source	$J_{max}^{eff,o}/K_{1/2}^s$ *	Source	A‡	$1/A$
0.079	All cell data	0.436	$C^{(i)} \leq 105$	0.0358 (0.0278)§	28.9 (36.0)
		0.402	$C^{(i)} \leq 70$ y-int = 0	0.0330 (0.0256)	30.3 (39.1)
0.070	Gluconate data only	0.436	$C^{(i)} \leq 105$	0.0314 (0.0244)	31.9 (41.0)
		0.402	$C^{(i)} \leq 70$ y-int = 0	0.0289 (0.0225)	34.6 (44.5)
0.085	Sucrose data only	0.436	$C^{(i)} \leq 105$	0.0383 (0.0296)	26.1 (33.7)
		0.402	$C^{(i)} \leq 70$ y-int = 0	0.0352 (0.0273)	28.4 (36.6)

*From slope of plot of $J^{eff,s}$ versus $C_{Cl}^{(i=o)}$, as in Fig. 5, determined by linear regression for the data range shown. Fits with the y-intercept fixed at 0 are indicated by y-int = 0. The values chosen represent the extremes of the slopes determined with different fitting conditions. ‡Calculated from Eq. 8 as described in *Theory*. §Corrected for modifier site inhibition as described in *Theory* (Eq. 10), using the observed mean $C_{Cl}^{(i)}$ and $K_I = 376$ mM.

inhibition by internal Cl^- are taken into account (Eq. 10), the values of A are somewhat lower, ranging from 0.023 to 0.030. Thus, the asymmetry of unloaded sites measured in this way is at least as pronounced as at 0°C.

Use of Flufenamic Acid (FA) to Test the Value of A

At 0°C with 150 mM $C_{Cl}^{(i=o)}$, 0.5–0.6 μM FA half-inhibits Cl^- exchange (Cousin and Motais, 1982; Knauf et al., 1989). FA does not compete with Cl^- for binding to the transport site, but its binding affinity is affected by the conformation of the transport site (inward or outward-facing, unloaded or loaded with substrate) (Knauf et al., 1989), making it a "mixed" inhibitor. The $E^{(o)}$ form has a 3.7-fold higher affinity for FA than does the $E^{(i)}$ form (Knauf et al., 1989). If FA affinity is also sensitive to transport site conformation at 38°C, FA can be used to test the value of A, as well as the ping-pong model itself.

Inhibition by Flufenamic Acid at 38°C

Fig. 6 *A* shows a semilogarithmic plot of ^{36}Cl efflux at 38°C from cells with 101.8 mM $C_{Cl}^{(i)}$ and 150 mM $C_{Cl}^{(o)}$. The slope of the best-fit straight line is equal to the rate-constant for ^{36}Cl exchange. The open circles represent control cells and the open triangles are for cells suspended in medium with 10 μM FA. Cl^- exchange is strongly inhibited in the presence of FA, but the IC_{50} is 7.6 μM, over 10-fold higher (less potent) than at 0°C.

Sidedness of FA Inhibition

Because FA has only a single charged group, which is a carboxylic acid, it, like other weak acids (Deuticke, 1982; Rothstein et al., 1974), may cross the red blood cell membrane in the uncharged acid form. Thus, the inhibitory FA binding site might face either the cytoplasm or the external medium. Some evidence at 0°C favors an external-facing site on band 3, because SITS (4-acetamido-4′-isothiocyano-stilbene-2,2′-disulfonate) and FA compete for binding (Cousin and Motais, 1982) and it is known that SITS binds to an external site.

To investigate the location of the FA site, we used ^{14}C-labeled FA to measure the rate at which FA crosses the membrane. The results, shown in Fig. 6 *B*, demonstrate that FA equilibrates rapidly across the membrane, regardless of whether or not nonradioactive FA is present at the opposite side, with a half-time of 19.2–21.5 ms.

Despite this rapid equilibration rate, FA does not equilibrate completely by ~50 msec, the time of the second Cl^- flux sample (Fig. 6 *A*) and therefore the first time at which Cl^- flux can be measured. If FA were acting at an intracellular site, the $^{36}Cl^-$ efflux (proportional to slope) measured from the first two open triangles in Fig. 6 *A*, where cells are first exposed to FA at time zero of the efflux measurement, should be larger than the Cl^- efflux seen when cells are pretreated with

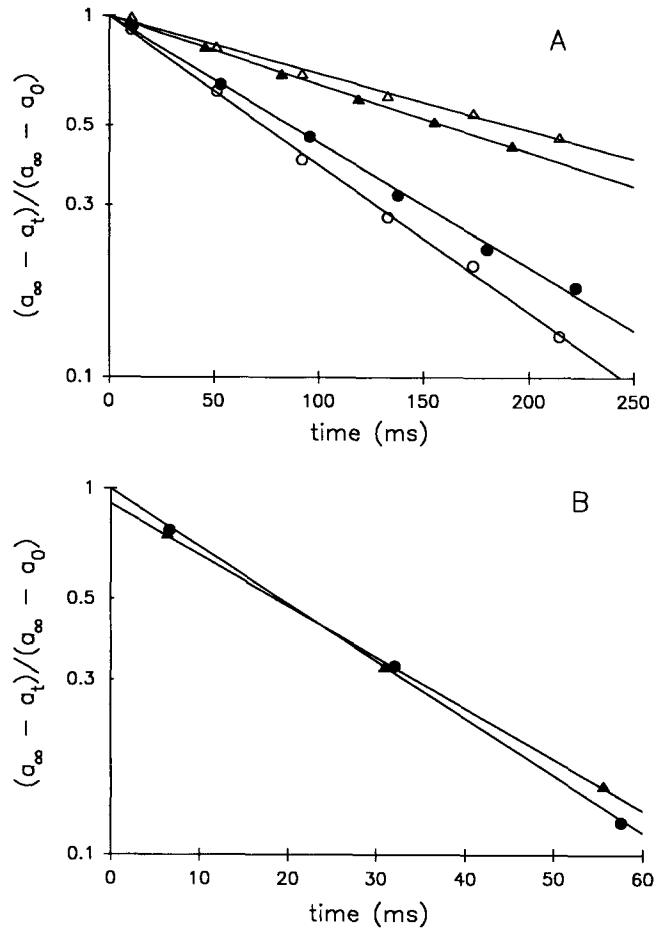

FIGURE 6. (*A*) ^{36}Cl efflux with or without FA. Cells had 101.8 ± 5.4 mM $C^{(i)}$ and were suspended in media with 150 mM $C^{(o)}$ at 38°C, pH 7.2. (*Circles*) no FA in medium; (*triangles*) 10 μM FA in medium. Solid symbols indicate that the cells were loaded with ^{36}Cl for ≥5 min in medium containing 10 μM FA. All flux media contained a total of 1% ethanol, the solvent used to dissolve FA. The cpm of ^{36}Cl in the medium (a_t) is plotted in a logarithmic fashion against time (see MATERIALS AND METHODS) so that the slope is equal to the rate constant for Cl^- efflux; a_0 = cpm at time zero; a_∞ = cpm after isotope equilibration. (*B*) ^{14}C-FA efflux with or without FA in the medium. (*Solid circles*) no FA in medium; (*solid triangles*) 10 μM FA in medium. Conditions identical to those in *A*, except that cells were loaded with ^{14}C-FA instead of ^{36}Cl, as described in MATERIALS AND METHODS.

FA, as in the solid triangles of Fig. 6 A. The fact that the ^{36}Cl efflux is nearly linear in both cases and is not more inhibited with FA pretreatment argues that the site of FA inhibition faces the external medium.

Mechanism of Inhibition by FA at 38°C

Although FA is a mixed inhibitor at 0°C, we wished to verify this at 38°C, particularly because in some ways FA resembles a competitive inhibitor at this temperature. For a competitive inhibitor, the x-intercept of a plot of

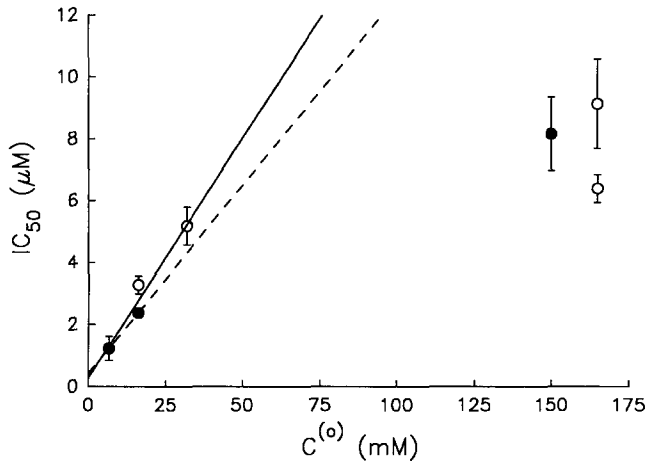

FIGURE 7. Dependence of IC_{50} for FA inhibition of Cl^- exchange on $C^{(o)}$ with constant $C^{(i)}$. Cells with $C^{(i)}$ of 110 mM (*solid circles*) or ghosts with $C^{(i)}$ of 177 mM (*open circles*) were suspended in media with various FA concentrations, and the concentration of FA that gives half inhibition (IC_{50}) was determined as described in MATERIALS AND METHODS. Bars indicate SEM if larger than the point size. The IC_{50} best-fit straight lines for $C^{(o)} \leq 32$ mM are shown for the intact cell data (*dashed line*) or for the combined data with ghosts and cells (*solid line*). The intercept at $C^{(o)} = 0$, which should be equal to K_e, the dissociation constant for FA binding to $E^{(o)}$, is 0.43 μM for the cell data, and 0.29 μM for the combined data.

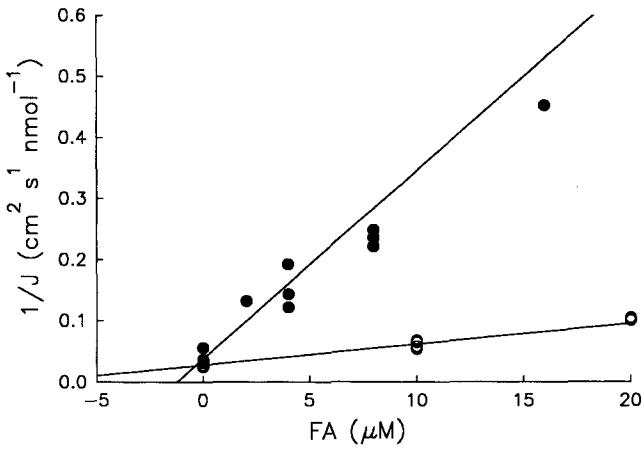

FIGURE 9. Dixon plot of effects of FA on unidirectional Cl^- efflux with constant $C^{(i)}$ and different $C^{(o)}$. Intact cells with 111.8 ± 9.2 mM $C^{(i)}$ were suspended in media with different concentrations of FA and with either 6.6 mM (*solid circles*) or 150 mM (*open circles*) $C^{(o)}$, with sucrose replacing Cl^-. Temperature was 38°C and pH was 7.2. The x-value of the intersection point of the lines for different $C^{(o)}$ (each determined by nonlinear fits to the flux versus [FA] data as described in MATERIALS AND METHODS) is equal to the negative of K_e, the dissociation constant for FA binding to $E^{(o)}$, which is 0.37 μM.

IC_{50} versus $C_{Cl}^{(o)}$ (Fig. 7) should be equal to $-K_{1/2}^{o}$ (Restrepo et al., 1991). The data for the two lowest $C_{Cl}^{(o)}$ for cells or ghosts fit this prediction well: for cells the x-intercept is −3.5 mM, and for the ghost and cell data, the x-intercept is −1.9 mM, both close to the negative of the $K_{1/2}^{o}$ obtained under similar circumstances, 3.01 mM for ghosts or 3.83 mM for cells. Thus, at low $C_{Cl}^{(o)}$, the IC_{50} for FA behaves very much as expected for a competitive inhibitor.[2] If, however, one fits a straight line to all of the data in Fig. 7, the x-intercept is −66

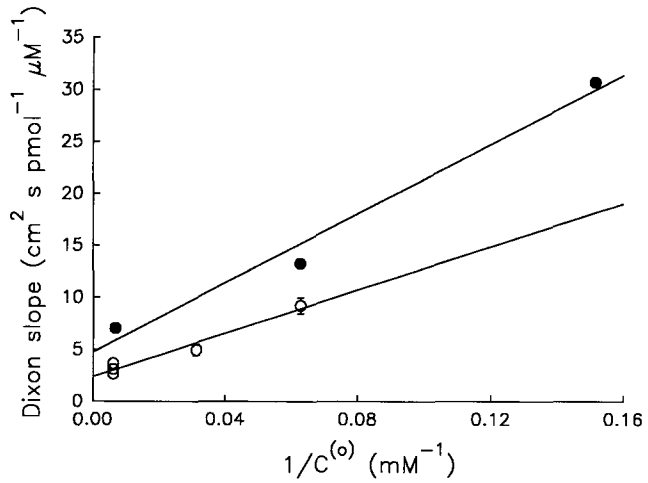

FIGURE 8. Plot of Dixon plot slope versus $1/C^{(o)}$. Cells (*solid circles*) or ghosts (*open circles*) with constant $C^{(i)}$ were exposed to FA and Dixon plots were constructed as in Fig. 9. The slopes of these plots are plotted against $1/C^{(o)}$. For the cells, the y-intercept is 4.8 ± 2.2 cm² · s · pmol⁻¹ · μM⁻¹, while for the ghosts, the intercept is 2.4 ± 0.6. The non-zero intercepts indicate that FA is not a competitive inhibitor.

[2]The dependence of IC_{50} on $C_{Cl}^{(o)}$ is nearly linear for low values of $C_{Cl}^{(o)}$ but the values of IC_{50} at $C_{Cl}^{(o)} \geq 150$ mM do not fit the line, indicating that IC_{50} tends to plateau at higher $C_{Cl}^{(o)}$ values. Very similar results are seen when $C_{Cl}^{(o)}$ is varied at 0°C (Knauf et al., 1989). This is the expected behavior for a mixed inhibitor which has a higher affinity for $E^{(o)}$ than for the other forms of band 3. The reciprocal of the IC_{50} is given by (Knauf et al., 1992):

$$1/IC_{50} = (1/K_e)\,(E^{(o)}/E_t) + (1/K_g)\,(E^{(i)}/E_t) + (1/K_f)\,(ECl^{(i)}/E_t) + (1/K_h)\,(ECl^{(o)}/E_t), \quad (3)$$

where K_e, K_f, K_g, and K_h are the dissociation constants for FA binding to the $E^{(o)}$, $ECl^{(o)}$, $E^{(i)}$, and $ECl^{(i)}$ forms of band 3, and E_t is the total amount of band 3, so $E^{(o)}/E_t$ etc. represent the fractions of band 3 in each form. At very low $C_{Cl}^{(o)}$, almost all of band 3 is in the $E^{(o)}$ form, so the first term dominates Eq. 13 and the IC_{50} approaches K_e. As $C_{Cl}^{(o)}$ increases, $E^{(o)}$ decreases (Fröhlich et al., 1983) and, since $E^{(o)}$ has the highest affinity for FA, the IC_{50} for FA must increase as the fraction of band 3 in the $E^{(i)}$, $ECl^{(i)}$, and $ECl^{(o)}$ forms increases, making the rightmost three terms in Eq. 13 more important in determining the overall IC_{50}.

The results in Fig. 7 show that a mixed inhibitor with a high affinity for $E^{(o)}$ can mimic the behavior of a competitive inhibitor in terms of the dependence of its IC_{50} on $C_{Cl}^{(o)}$ in the region of low $C_{Cl}^{(o)}$, so such data do not provide convincing evidence concerning the nature of the inhibition. Data at higher $C_{Cl}^{(o)}$ or Dixon slope data are required to make this distinction. Note that if $K_e \ll K_f$, K_g, and K_h, the IC_{50} may vary linearly with $C_{Cl}^{(o)}$ up to quite high values of $C_{Cl}^{(o)}$.

TABLE III

Dissociation Constants for FA Binding to Band 3 at 0°C and 38°C

	0°C	38°C	38°C/0°C	ΔH^{app}
K_e (E_o)	0.083 μM* ±0.005	0.29–0.43 μM‡	3.5–5.2	23.3–30.6§
K_g (E_i)	0.03 μM* ±0.05	10.4 μM‖	34.7	65.9
K_g/K_e	3.7	24–36	6.7–10	

*From (Knauf et al., 1989). ‡From combined data for cells and ghosts or from cell data of Fig. 7, respectively. The value from the intersection point of Fig. 9, 0.37 μM, lies between these values. §ΔH in kJ/mol. ‖From Fig. 10.

mM, far different from that expected for competitive inhibition.

Further evidence that FA is not a competitive inhibitor comes from an analysis of the dependence of the Dixon plot slope on $1/C_{Cl}^{(o)}$ (Fig. 8). For a competitive inhibitor, the points should fall on a straight line which has a zero y-intercept (Restrepo et al., 1991). The y-intercepts for the data with ghosts (2.4 ± 0.6 $cm^2 \cdot s \cdot pmol^{-1} \cdot \mu M^{-1}$) or cells (4.8 ± 2.2 $cm^2 \cdot s \cdot pmol^{-1} \cdot \mu M^{-1}$) are both different from zero, indicating that FA is a mixed or noncompetitive inhibitor.

Determination of FA Affinity for the $E^{(o)}$ Form of Band 3

Fig. 9 shows Dixon plots for cells with 111.8 mM $C_{Cl}^{(i)}$ suspended in medium with 150 mM $C_{Cl}^{(o)}$ or 6.6 mM $C_{Cl}^{(o)}$. As described previously (Fröhlich and Gunn, 1986; Knauf et al., 1987), the negative of the x-value of the intersection point of the two lines with different $C_{Cl}^{(o)}$ gives K_e, the dissociation constant for FA binding to $E^{(o)}$. Because K_e is so low (0.37 μM), it is not determined very precisely, but it is clearly less than the IC_{50} for 6.6 mM $C_{Cl}^{(o)}$, given by the negative of the x-intercept, which is 1.23 ± 0.38 μM.

Another way of determining K_e is to extrapolate the IC_{50} values for FA with different low $C_{Cl}^{(o)}$ to zero $C_{Cl}^{(o)}$ (Fröhlich and Gunn, 1986). Fig. 7 shows data for cells with an average $C_{Cl}^{(i)}$ of 110 mM (*solid circles*) and for ghosts with an average $C_{Cl}^{(i)}$ of 177 mM (*open circles*). Extrapolation of the two low $C_{Cl}^{(o)}$ points for cells to zero $C_{Cl}^{(o)}$ gives a K_e value of 0.43 μM. If the data for cells and ghosts at low $C_{Cl}^{(o)}$ are combined, the K_e is 0.29 μM. Both of these values are close to that obtained from the intersection point of the Dixon plot lines in Fig. 9 (0.37 μM). Although these data do not define a statistical lower limit for K_e at 38°C, the K_e value appears to be over three times higher than at 0°C (Table III), even if the lowest experimental value is chosen, indicating that the affinity of $E^{(o)}$ for FA probably decreases with increasing temperature.

Determination of FA Affinity for the $E^{(i)}$ Form of Band 3

The dissociation constant for FA binding to the $E^{(i)}$ form of band 3 (with the transport site facing inward and unloaded), K_g, can be obtained in a fashion similar to that used in Fig. 9 to determine K_e. In this case, Dixon plots for FA inhibition are constructed for conditions with $C_{Cl}^{(o)}$ constant and with $C_{Cl}^{(i)}$ varied (Fig. 10). The negative of the x-value of the intersection point of the lines with different $C_{Cl}^{(i)}$ is equal to K_g. From the data in Fig. 10, K_g is 10.4 μM, far greater than K_e.

K_g at 38°C is nearly 35 times higher than the value at 0°C (Table III), indicating an even larger temperature dependence than for K_e. More importantly, the ratio of

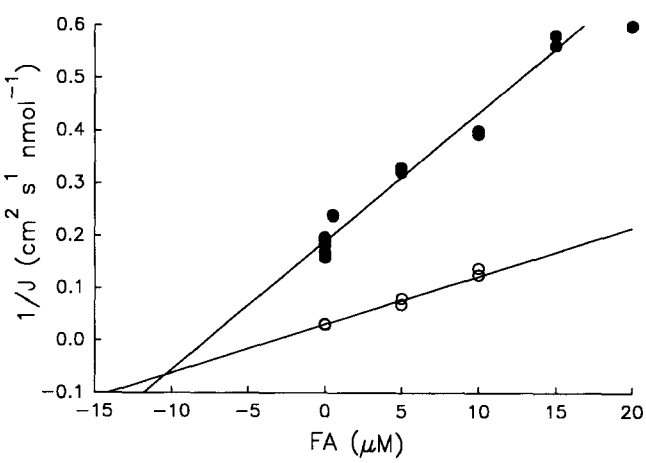

FIGURE 10. Determination of K_g for FA. Resealed ghosts with constant $C^{(o)}$ of 16 mM and with $C^{(i)}$ either 16 mM (*solid circles*) or 171 mM (*open circles*) were exposed to FA and the reciprocal of the unidirectional Cl^- efflux was plotted against the FA concentration. The intersection point of the lines for different $C^{(i)}$ (determined as described for Fig. 9) is equal to the negative of K_g, the dissociation constant for FA binding to $E^{(i)}$, which is 10.4 μM.

TABLE IV

Determination of Asymmetry from FA Inhibition Data

IC_{50}^{0Cl}	Source	K_g	K_e	A*	$1/A$
7.69 μM‡ ±1.15	$C^{(i=o)}$ 16 mM				
7.69 μM‡ ±0.75	$C^{(i=o)}$ 165 mM	10.4§	0.29‖	0.010	97.9
			1.23¶	0.050	20.2
7.73 μM**	Dixon plot intersection	10.4§	0.29‖	0.010	99.9
			1.23¶	0.049	20.6

*Calculated from Eq. 12. ‡IC_{50} measured at the indicated $C_{Cl}^{(i=o)}$. Because the IC_{50} values are equal for the two $C_{Cl}^{(i=o)}$, they are identical to the extrapolated IC_{50}^{0Cl}. §From Fig. 10. ‖From combined ghost and cell data in Fig. 7. ¶From x-intercept for 6.6 mM $C_{Cl}^{(o)}$ in Fig. 9. **From Fig. 11.

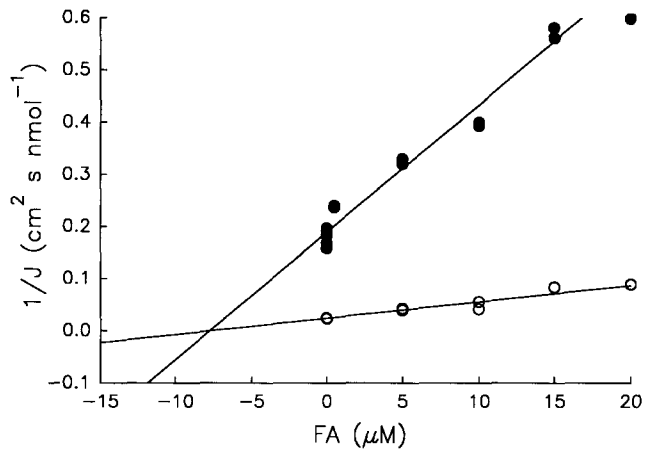

FIGURE 11. Determination of IC_{50}^{0Cl} for FA. The concentration of FA required to half-inhibit Cl^- exchange under symmetric conditions as $C^{(i=o)}$ approaches zero, IC_{50}^{0Cl}, is given by the negative of the x-value of the intersection point of the Dixon plot (1/flux, J, versus FA concentration) lines for ghosts with $C^{(i=o)}$ of 16 mM and 165 mM, and is 7.73 μM.

K_g to K_e at 38°C is 24–36, far larger than the ratio of 3.7 at 0°C (Knauf et al., 1989). The fact that the affinity of band 3 for FA is so strongly dependent on the conformation of the transport site ($E^{(o)}$ or $E^{(i)}$) means that the IC_{50} for FA can provide very useful information on the fraction of band 3 in the $E^{(o)}$ and $E^{(i)}$ forms and hence on the asymmetry factor, A.

Determination of A from IC_{50} for FA

For an inhibitor (like FA) that is not competitive, Fröhlich and Gunn (1986) have shown that the IC_{50} extrapolated to zero $C_{Cl}^{(i=o)}$, IC_{50}^{0Cl}, can be expressed in terms of A, K_e, and K_g, and that this equation can be solved for A to give:

$$A = (1 - IC_{50}^{0Cl}/K_g)/(IC_{50}^{0Cl}/K_e - 1). \qquad (12)$$

The average IC_{50} values in ghosts with either 16 mM $C_{Cl}^{(i=o)}$ or 165 mM $C_{Cl}^{(i=o)}$ are identical (Table IV), making it easy to extrapolate to zero $C_{Cl}^{(i=o)}$. (A similarly constant IC_{50} as a function of $C_{Cl}^{(i=o)}$ is seen at 0°C for the close analogue of FA, niflumic acid (Cousin and Motais, 1979), but not for FA itself (Knauf et al., 1989).) Using different estimates for K_e, the calculated A values (Table IV) range from 0.01 to 0.05, indicating asymmetry strongly in favor of inward-facing sites, in agreement with the Cl^- half-saturation experiments (Tables I and II).

For a mixed inhibitor such as FA, Fröhlich and Gunn (1986) have also shown that the negative of the x-value of the intersection point for Dixon plots with different $C_{Cl}^{(i=o)}$ is identical to the IC_{50}^{0Cl}. Fig. 11 shows such a plot, from which the x-coordinate of the intersection point is −7.73 μM. This is very close to the value determined by extrapolation of IC_{50} to zero $C_{Cl}^{(i=o)}$, so the corresponding A values (Table IV) again are consistent with the results from Cl^- half-saturation experiments.

DISCUSSION

Effects of Ionic Strength and Membrane Potential on Measurements

When $C_{Cl}^{(o)}$ is varied at constant $C_{Cl}^{(i)}$, the membrane potential changes, because for red cells V_m is very close to the Nernst potential for chloride. Jennings et al. (1990) and others (Gunn and Fröhlich, 1979; Fröhlich, 1984; Wieth et al., 1980) have found that there is little or no effect of V_m on human red cell anion transport or on binding of monovalent anions at 0°C, so it seems unlikely that V_m has any large effects at 38°C. Another possibility is that changes in the external ionic strength might affect Cl^- flux in the experiments where $C_{Cl}^{(o)}$ is replaced by sucrose, but the similar results when ionic strength was maintained with gluconate or citrate (Fig. 2) argue strongly that external ionic strength has no significant effect.

When $C_{Cl}^{(i=o)}$ is varied, V_m remains constant at zero, but there are considerable changes in ionic strength. Although previous work (Gunn and Fröhlich, 1979) at 0°C provides some evidence against pronounced ionic strength effects, the parameters obtained should be regarded as "apparent" values, whose validity is limited to the conditions used here.

Comparison of $K_{1/2}$ Values with Other Determinations

$K_{1/2}^o$ is well-determined from the MM fits to the data (Figs. 1–3). In contrast, the determination of $K_{1/2}^s$ is much more difficult, due to the flat maximum and the scatter in the data (Fig. 4). The MM model provides an adequate fit to the data for $C_{Cl}^{(i=o)} \leq 500$ mM, with $K_{1/2}^s = 106$ mM, but the slightly better fit of the MS or CMS models suggests that $K_{1/2}^s$ might be as large as 375 mM. For bicarbonate, $K_{1/2}^s$ is 173 mM (Gasbjerg et al., 1996). Thus, neither Cl^- nor bicarbonate seems to have a very high affinity for the anion exchanger under symmetric conditions at 38°C.

Since $K_{1/2}^o$ is very low, and $K_{1/2,max}^o + K_{1/2,max}^i = K_{1/2}^s$ (Fröhlich and Gunn, 1986), $K_{1/2}^s$ must be $\approx K_{1/2,max}^i$. Thus, under physiological conditions, the anion exchanger is largely saturated at the outside, but is not completely saturated at the inside. At either side of the membrane, however, a step increase in the ratio of HCO_3^- to Cl^- will cause a nearly linear change in the relative fluxes of the two ions, as required for the physiologically necessary anion exchange.

Brahm (1977) previously reported a $K_{1/2}^s$ value of

about 65 mM at 38°C.[3] This value, however, was obtained in the presence of NH_4Cl, which inhibits transport and may alter the parameters of the system. Glibowicka et al. (1988) have used nuclear magnetic resonance (NMR) line-broadening to obtain a value of 49 ± 11 mM at 42°C, in ghosts prepared with 20 mM EDTA. Although this approach has merit, because such NMR measurements are not affected by interactions of Cl^- with the modifier site (Falke and Chan, 1985), recent NMR studies with higher magnetic fields indicate that the free induction decay of the NMR signal for ^{35}Cl has a double exponential time course (Liu et al., 1996; Price et al., 1991), rather than a single exponential as assumed by Glibowicka et al. Since their measurements of line-broadening were also done with a fairly high field, their fits of the peaks to a Lorentzian function (which assumes a single exponential decay), may contain a systematic error, that could substantially affect the value of $K_{1/2}^s$ obtained.[4] A possible problem with NMR determinations of affinity is suggested by Galanter and Labotka's (1991) observation that direct ^{35}Cl NMR gave a $K_{1/2}^s$ value of 74 ± 10 mM at 21°C, but Cl^- competition experiments using ^{14}N-nitrate NMR gave a much lower $K_{1/2}^s$ of 10.3 ± 1.1 mM; the reason for this discrepancy is unknown.

Comparison to Predictions of the Ping-pong Model

According to the ping-pong model for anion exchange, the unloaded site asymmetry factor, A ($=E^{(i)}/E^{(o)}$ with $C_{Cl}^{(i)} = C_{Cl}^{(o)}$), should be the same regardless of the anion substrate which is used to measure it, because A reflects the free energy difference (ΔG) between the unloaded inward- and outward-facing forms ($E^{(i)}$ and $E^{(o)}$) of capnophorin. The values of A obtained from the chloride flux data presented in Table I range between 0.038 and 0.107, while those in Table II lie between 0.023 and 0.038. Most of these values are slightly lower than the values of 0.10–0.13 obtained from bicarbonate flux data in the preceding paper (Gasbjerg et al., 1996). The significance of this difference, however, must be tempered by the realization that determinations of A involve several experimental measurements, some of which are subject to considerable error. For example, the bicarbonate A value may be affected by the uncertainty in $K_{1/2}^s$ because of modifier site inhibition; if $K_{1/2}^s$ were slightly higher, A would be lower and thus closer to the values from the Cl^- data in this paper. In the case of the chloride data, the $J_{max}^{eff,s}/K_{1/2}^s$ value is given by the initial slope with very low Cl^-, but the actual measurements could not be performed below 16 mM $C_{Cl}^{(i=o)}$, so it is possible that the slope is underestimated, particularly if $K_{1/2}^s$ is low as indicated by the MM fits. (Note difference in $J_{max}^{eff,s}/K_{1/2}^s$ values between Tables I and II). Although the linearity of the flux versus $C_{Cl}^{(i=o)}$ plot (Fig. 5) argues against this possibility, because of scatter one cannot rule out a somewhat nonlinear dependence of flux on $C_{Cl}^{(i=o)}$ over the range from 16 to 100 mM. An underestimate of $J_{max}^{eff,s}/K_{1/2}^s$ would give an artificially low A value, which would explain much of the difference between the A values for chloride and bicarbonate.

The calculated ΔG between the $E^{(o)}$ and $E^{(i)}$ forms from the chloride A values (Tables I and II) is 5.8–9.5 kJ/mol, similar to the value of 5.3–6 kJ/mol obtained from the bicarbonate A values at 38°C (Gasbjerg et al., 1996). Both A values indicate that the $E^{(i)}$ form of capnophorin has a much lower free energy than does the $E^{(o)}$ form.

Despite the differences in the asymmetry values calculated for the chloride and bicarbonate flux data, it should be emphasized that in each case, the ping-pong model provides a self-consistent interpretation of all of the flux data.

Another and even more independent test of the ping-pong model is provided by the flufenamic acid studies. Because FA exhibits such a strong preference (24–36-fold, Table III) for the $E^{(o)}$ over the $E^{(i)}$ conformation, FA provides a very powerful tool for analyzing the fraction of capnophorin in each conformation. Various methods for estimating the affinities of FA for $E^{(i)}$ and $E^{(o)}$, as well as for determining the IC_{50} at zero chloride (Table IV), give A values ranging from 0.01 to 0.05. These agree fairly well with the chloride A values (0.023 to 0.107), but are somewhat lower than the values obtained with bicarbonate (0.10 to 0.13).[5] The fact that there is reasonable agreement between A as determined by fluxes or by FA inhibition demonstrates the predictive power of the ping-pong model and thus pro-

[3]If all of the data are fitted to a simple MM equation, however, as in Fig. 4 *A*, *solid line* (the same procedure used by Brahm [1977]), $K_{1/2}^s$ is only 60 mM, similar to the value obtained by Brahm. Because of the uncertainty in fitting the MS model to the data, this value (60 mM) should probably be regarded as the lowest $K_{1/2}^s$ value that is compatible with the data at 38°C. Because of the relatively poor fit of the MM equation to the data in Fig. 4 *A*, the true $K_{1/2}^s$ value is likely to be higher, but it is difficult to say exactly how much higher.

[4]Even if the $K_{1/2}^s$ value of 49 mM from Glibowicka et al. (1988) were used together with our $K_{1/2}^o$ value, A would be only 0.12, near the range of values observed in this and the accompanying (Gasbjerg et al., 1996) paper and consistent with the concept that the asymmetry is similar at low and high temperature.

[5]The FA inhibitory potency provides a very strong test of the direction of asymmetry, but does not give a very accurate value for A if A is either very small or very large. In either case, the IC_{50}^{0Cl} value approaches either K_c or K_g, and so small errors in the determination of these parameters give rise to large variations in A. For the case of capnophorin, A is very small so K_g and IC_{50}^{0Cl} are similar; since neither is determined to great precision, some deviations from the predictions of the ping-pong model are to be expected.

vides strong evidence that this model is a basically correct description of the transport mechanism.

Relation to Predicted Temperature Effects on the Asymmetry

As discussed in the preceding paper (Gasbjerg et al., 1996), Glibowicka et al. (1988) have proposed an explanation of the curvilinear temperature dependence of anion exchange that involves a change in asymmetry of the system, so that the rate constant (k) for outward translocation ($ECl^{(i)}$ to $ECl^{(o)}$) is rate-limiting at low temperature ($k < k'$), but the rate constant (k') for the transition from $ECl^{(o)}$ to $ECl^{(i)}$ becomes rate-limiting at high temperature. Based on Glibowicka et al.'s calculations and their assumptions that temperature has little effect on the ion binding constants, K_o and K_i, A should increase by over sevenfold from 0 to 38°C (because of the increase in k/k'). Both the flux data for chloride and bicarbonate (Gasbjerg et al., 1996) and the estimates of asymmetry using FA clearly demonstrate that A at 38°C is approximately as small as or smaller than the value measured at 0°C, that is, that the asymmetry in favor of inward-facing unloaded sites either stays the same or increases with increasing temperature. This provides very strong evidence against the hypothesis of Glibowicka et al., although the data do not rule out alternate possibilities in which the ion affinities change (because $A = kK_o/k'K_i$). Parenthetically, it is interesting to note that when external pH is increased, there is a reversal of A so that more unloaded sites face outward than inward (Bjerrum, 1992). This is in strong contrast to the lack of effect of temperature on A, and probably reflects decreases in the affinity of the external-facing transport site for anions, resulting from titration of positive charges near the site.

Relation to Physiological Anion Exchange

The data in this paper, together with those in the preceding paper (Gasbjerg et al., 1996), provide information that can be used to determine the rate of exchange of chloride for bicarbonate under various physiological conditions. Interestingly, the transport properties of capnophorin at body temperature seem to be considerably different from those at 0°C. In particular, the system does not seem to be fully saturated at the cytoplasmic side of the membrane. In view of evidence that the binding and dissociation reactions for chloride at the interfaces are not rate-limiting, there seems to be no advantage in having more unloaded transport sites. One possibility not yet ruled out, however, is that one of the debinding reactions for bicarbonate might under some conditions limit the rate of chloride-bicarbonate exchange. If the off reaction for bicarbonate at the inside were rate-limiting, there might be some advantage to having a system with excess capacity to bind and transport chloride from inside to outside. Further studies of the reactions involving bicarbonate are required to test this possibility.

Mrs. Birgitte D. Olsen and Mrs. Lise Mikkelsen are gratefully thanked for their skillful technical help, as well as Dr. Poul Bjerrum for helpful discussions.

J. Brahm was the recipient of an Alfred Benzon Senior Investigator Fellowship, and P. Knauf was supported by a Fogarty Senior International Fellowship (TW00975) from the U.S. Public Health Service. The financial support from NOVO's Fond, from the Weimann Foundation, and from the National Institutes of Health through grant DK27495 is gratefully acknowledged.

Original version received 18 August 1995 and accepted version received 16 September 1996.

REFERENCES

Bjerrum, P.J. 1992. The human erythrocyte anion transport protein, band 3. Characterization of exofacial alkaline titratable groups involved in anion binding/translocation. *J. Gen. Physiol.* 100:301–339.

Brahm, J. 1977. Temperature-dependent changes of chloride transport kinetics in human red cells. *J. Gen. Physiol.* 70:283–306.

Brahm, J. 1982. Diffusional water permeability of human erythrocytes and their ghosts. *J. Gen. Physiol.* 79:791–819.

Brahm, J. 1989. Transport measurement of anions, nonelectrolytes and water in red blood cell and ghost systems. *In* Methods in Enzymology. B. Fleischer and S. Fleischer, editors. Academic Press, New York. 160–175.

Cabantchik, Z.I., and A. Rothstein. 1974. Membrane proteins related to anion permeability of human red blood cells. I. Localization of disulfonic stilbene binding sites in proteins involved in permeation. *J. Membr. Biol.* 15:207–226.

Cousin, J.L., and R. Motais. 1979. Inhibition of anion permeability by amphiphilic compounds in human red cell: evidence for an interaction of niflumic acid with the band 3 protein. *J. Membr. Biol.* 46:125–153.

Cousin, J.L., and R. Motais. 1982. Inhibition of anion transport in the red blood cell by anionic amphiphilic compounds. I. Determination of the flufenamate-binding site by proteolytic dissection of the band 3 protein. *Biochim. Biophys. Acta.* 687:147–155.

Dalmark, M. 1976. Effects of halides and bicarbonate on chloride transport in human red blood cells. *J. Gen. Physiol.* 67:223–234.

Dalmark, M., and J.O. Wieth. 1972. Temperature dependence of chloride, bromide, iodide, thiocyanate and salicylate transport in human red cells. *J. Physiol. (Lond.).* 224:583–610.

Deuticke, B. 1982. Monocarboxylate transport in erythrocytes. *J. Membr. Biol.* 70:89–103.

Falke, J.J., and S.I. Chan. 1985. Evidence that anion transport by

band 3 proceeds via a ping-pong mechanism involving a single transport site. A ^{35}Cl NMR study. *J. Biol. Chem.* 260:9537–9544.

Fröhlich, O. 1984. Relative contributions of the slippage and tunneling mechanisms to anion net efflux from human erythrocytes. *J. Gen. Physiol.* 84:877–893.

Fröhlich, O., and R.B. Gunn. 1986. Erythrocyte anion transport: the kinetics of a single-site obligatory exchange system. *Biochim. Biophys. Acta.* 864:169–194.

Fröhlich, O., C. Leibson, and R.B. Gunn. 1983. Chloride net efflux from intact erythrocytes under slippage conditions. Evidence for a positive charge on the anion binding/transport site. *J. Gen. Physiol.* 81:127–152.

Funder, J., and J.O. Wieth. 1976. Chloride transport in human erythrocytes and ghosts: a quantitative comparison. *J. Physiol. (Lond.).* 262:679–698.

Galanter, W.L., and R.J. Labotka. 1991. The binding of nitrate to the human anion exchange protein (AE1) studied with ^{14}N nuclear magnetic resonance. *Biochim. Biophys. Acta.* 1079:146–151.

Gasbjerg, P.K., and J. Brahm. 1991. Kinetics of bicarbonate and chloride transport in human red cell membranes. *J. Gen. Physiol.* 97:321–350.

Gasbjerg, P.K., P.A. Knauf, and J. Brahm. 1996. Kinetics of bicarbonate transport in human red blood cell membranes at body temperature. *J. Gen. Physiol.* 108:565–575.

Glibowicka, M., B. Winckler, N. Aranibar, M. Schuster, H. Hanssum, H. Rüterjans, and H. Passow. 1988. Temperature dependence of anion transport in the human red blood cell. *Biochim. Biophys. Acta.* 946:345–358.

Gunn, R.B., and O. Fröhlich. 1979. Asymmetry in the mechanism for anion exchange in human red blood cell membranes. Evidence for reciprocating sites that react with one transported anion at a time. *J. Gen. Physiol.* 74:351–374.

Hunter, M.J. 1971. A quantitative estimate of the non-exchange-restricted chloride permeability of the human red cell. *J. Physiol. (Lond.).* 218:49P–50P. (Abstr.).

Hunter, M.J. 1977. Human erythrocyte anion permeabilities measured under conditions of net charge transfer. *J. Physiol. (Lond.).* 268:35–49.

Jennings, M.L. 1982. Stoichiometry of a half-turnover of band 3, the chloride transport protein of human erythrocytes. *J. Gen. Physiol.* 79:169–185.

Jennings, M.L. 1992*a*. Cellular anion transport. *In* The Kidney: Physiology and Pathophysiology. D.W. Seldin and G. Giebisch, editors. Raven Press, New York. 113–145.

Jennings, M.L. 1992*b*. Anion transport proteins. *In* The Kidney: Physiology and Pathophysiology. D. W. Seldin and G. Giebisch, editors. Raven Press, New York. 503–535.

Jennings, M.L., M. Allen, and R.K. Schulz. 1990. Effect of membrane potential on electrically silent transport: potential-independent translocation and asymmetric potential-dependent substrate binding to the red blood cell anion exchange protein. *J. Gen. Physiol.* 96:991–1012.

Knauf, P.A. 1986. Anion transport in erythrocytes. *In* Membrane Transport Disorders. T.E. Andreoli, S.G. Schultz, J.F. Hoffman, and D.D. Fanestil, editors. Plenum, New York. 191–220.

Knauf, P.A. 1989. Kinetics of anion transport. *In* The Red Cell Membrane. B.U. Raess and G. Tunnicliff, editors. Humana Press, Clifton, N.J. 171–200.

Knauf, P.A., and J. Brahm. 1989. Functional asymmetry of the anion exchange protein, capnophorin: effects on substrate and inhibitor binding. *In* Methods in Enzymology, Vol. 173. S. Fleischer and B. Fleischer, editors. Academic Press, New York. 432–453.

Knauf, P.A., and N.A. Mann. 1986. Location of the chloride self-inhibitory site of the human erythrocyte anion exchange system. *Am. J. Physiol.* 251:C1–C9.

Knauf, P.A., N.A. Mann, J.E. Kalwas, L.J. Spinelli, and M. Ramjeesingh. 1987. Interactions of NIP-taurine, NAP-taurine, and Cl^- with the human erythrocyte anion exchange system. *Am. J. Physiol.* 253:C652–C661.

Knauf, P.A., D. Restrepo, S.J. Liu, N.M. Raha, L.J. Spinelli, Y. Law, B. Cronise, R.B. Snyder, and L. Romanow. 1992. Mechanisms of substrate binding, inhibitor binding, and ion translocation in band 3 and band 3-related proteins. *Prog. Cell Res.* 2:35–44.

Knauf, P.A., L.J. Spinelli, and N.A. Mann. 1989. Flufenamic acid senses conformation and asymmetry of human erythrocyte band 3 anion transport protein. *Am. J. Physiol.* 257:C277–C289.

Kopito, R.R. 1990. Molecular biology of the anion exchanger gene family. *Int. Rev. Cytol.* 123:177–199.

Liu, D., P.A. Knauf, and S.D. Kennedy. 1996. Detection of Cl^- binding to band 3 by double-quantum-filtered ^{35}Cl nuclear magnetic resonance. *Biophys. J.* 70:715–722.

Lux, S.E., K.M. John, R.R. Kopito, and H.F. Lodish. 1989. Cloning and characterization of band 3, the human erythrocyte anion-exchange protein (AE1). *Proc. Natl. Acad. Sci. USA.* 86:9089–9093.

Passow, H. 1986. Molecular aspects of band 3 protein-mediated anion transport across the red blood cell membrane. *Rev. Physiol. Biochem. Pharmacol.* 103:61–223.

Passow, H., H. Fasold, L. Zaki, B. Schuhmann, and S. Lepke. 1974. Membrane proteins and anion exchange in human erythrocytes. *In* Biomembranes: Structure and Function. G. Gardos and I. Szasz, editors. North-Holland Publishing Company, Amsterdam. 197–214.

Price, W.S., P.W. Kuchel, and B.A. Cornell. 1991. A ^{35}Cl and ^{37}Cl NMR study of chloride binding to the erythrocyte anion transport protein. *Biophys. Chem.* 40:329–337.

Restrepo, D., B.L. Cronise, R.B. Snyder, L.J. Spinelli, and P.A. Knauf. 1991. Kinetics of DIDS inhibition of HL-60 cell anion exchange rules out ping-pong model with slippage. *Am. J. Physiol.* 260:C535–C544.

Rothstein, A., P.A. Knauf, Z.I. Cabantchik, and M. Balshin. 1974. The location and chemical nature of drug "targets" within the human erythrocyte membrane. *In* Drugs and Transport Processes. B.A. Callingham, editor. The Macmillan Press, London. 53–72.

Tanner, M.J.A., P. Martin, and S. High. 1988. The complete amino acid sequence of the human erythrocyte membrane anion-transport protein deduced from the cDNA sequence. *Biochem. J.* 256: 703–712.

Wieth, J.O., and P.J. Bjerrum. 1983. Transport and modifier sites in capnophorin, the anion transport protein of the erythrocyte membrane. *In* Structure and Function of Membrane Proteins. E. Quagliariello and F. Palmieri, editors. Elsevier Science Publishers B.V., 95–106.

Wieth, J.O., J. Brahm, and J. Funder. 1980. Transport and interactions of anions and protons in the red blood cell membrane. *Ann. NY Acad. Sci.* 341:394–418.